



Locations and contributions of the phosphotransferases EPT1 and CEPT1 to the biosynthesis of ethanolamine phospholipids^S

Yasuhiro Horibata, Hiromi Ando, and Hiroyuki Sugimoto¹

Department of Biochemistry, Dokkyo Medical University School of Medicine, Mibu, Tochigi 321-0293, Japan

Abstract The final step of the CDP-ethanolamine pathway is catalyzed by ethanolamine phosphotransferase 1 (EPT1) and choline/EPT1 (CEPT1). These enzymes are likely involved in the transfer of ethanolamine phosphate from CDP-ethanolamine to lipid acceptors such as 1,2-diacylglycerol (DAG) for PE production and 1-alkyl-2-acyl-glycerol (AAG) for the generation of 1-alkyl-2-acyl-glycerophosphoethanolamine. Here, we investigated the intracellular location and contribution to ethanolamine phospholipid (EP) biosynthesis of EPT1 and CEPT1 in HEK293 cells. Immunohistochemical analyses revealed that EPT1 localizes to the Golgi apparatus and CEPT1 to the ER. We created EPT1-, CEPT1-, and EPT1-CEPT1-deficient cells, and labeling of these cells with radio- or deuterium-labeled ethanolamine disclosed that EPT1 is more important for the de novo biosynthesis of 1-alkenyl-2-acyl-glycerophosphoethanolamine than is CEPT1. EPT1 also contributed to the synthesis of PE species containing the fatty acids 36:1, 36:4, 38:5, 38:4, 38:3, 40:6, 40:5, and 40:4. In contrast, CEPT1 was important for PE formation from shorter fatty acids such as 32:2, 32:1, 34:2, and 34:1. Brefeldin A treatment did not significantly affect the levels of the different PE species, indicating that the subcellular localization of the two enzymes is not responsible for their substrate preferences. In vitro enzymatic analysis revealed that EPT1 prefers AAG 16–20:4 > DAG 18:0–20:4 > DAG 16:0–18:1 = AAG 16–18:1 as lipid acceptors and that CEPT1 greatly prefers DAG 16:0–18:1 to other acceptors. ^S These results suggest that EPT1 and CEPT1 differ in organelle location and are responsible for the biosynthesis of distinct EP species.—Horibata, Y., H. Ando, and H. Sugimoto. Locations and contributions of the phosphotransferases EPT1 and CEPT1 to the biosynthesis of ethanolamine phospholipids. *J. Lipid Res.* 2020. 61: 1221–1231.

Supplementary key words phosphatidylethanolamine • phosphatidylcholine • plasmalogens • phospholipid biosynthesis • phospholipid metabolism • ethanolamine phosphotransferase 1 • choline/ethanolamine phosphotransferase 1 • Kennedy pathway

This work was supported in part by Japan Society for the Promotion of Science KAKENHI Grant 17K08642 (Y.H.), the Yamada Science Foundation (Y.H.), the Takeda Science Foundation (Y.H.), and the Ichiro Kanehara Foundation (Y.H.). The authors declare that they have no conflicts of interest with the contents of this article.

Manuscript received 11 May 2020 and in revised form 17 June 2020.

Published, *JLR Papers in Press*, June 23, 2020
DOI <https://doi.org/10.1194/jlr.RA120000898>

Copyright © 2020 Horibata et al. Published under exclusive license by The American Society for Biochemistry and Molecular Biology, Inc.
This article is available online at <https://www.jlr.org>

Ethanolamine phospholipid (EP) in mammalian cells mainly comprises PE. In many cells and tissues, PE is the second most abundant phospholipid after PC and generally constitutes approximately 20–40% of cellular phospholipids (1). PE is composed of DAG and ethanolamine phosphate. Another type of EP found in mammalian cells is ether-linked lipid such as 1-alkyl-2-acyl-glycerophosphoethanolamine (plasmanyl-PE) and 1-alkenyl-2-acyl-glycerophosphoethanolamine (plasmenyl-PE), also called plasmalogen. Lipid moieties of these EPs are 1-alkyl-2-acyl-glycerol (AAG) and 1-alkenyl-2-acyl-glycerol, respectively. In mammals, 20% of total phospholipids have ether-linkage, but quantity of the lipid varies from tissue to tissue. In human brain, plasmenyl-PE is the main EP (up to 80% of total EP). The lipid is also found in heart, lung, kidney, spleen, skeletal muscle, and testis. Liver contains plasmenyl-PE as less than 1% of the total phospholipids. Generally, the 1-alkenyl group is present in plasmenyl-PE, whereas the 1-alkyl group is present in 1-alkyl-2-acyl-glycerophosphocholine (plasmanyl-PC). The content of plasmanyl-PC is highest in heart and skeletal muscle and is low in other organs.

Figure 1 shows the biosynthetic pathway and subcellular location for synthesis of PE, plasmanyl-PE, and plasmenyl-PE in mammalian cells. PE is mainly synthesized by two pathways: the PS decarboxylation pathway and the CDP-ethanolamine pathway (or Kennedy pathway) (Fig. 1A) (2). In the PS decarboxylation pathway, the serine base in PS is decarboxylated by PS decarboxylase (PSD) to generate PE on the mitochondrial inner membrane. The PS

Abbreviations: AAG, 1-alkyl-2-acyl-glycerol; BFA, brefeldin A; CEPT1, choline/ethanolamine phosphotransferase 1; DHAP, dihydroxyacetone phosphate; DKO, double-KO; EP, ethanolamine phospholipid; EPT1, ethanolamine phosphotransferase 1; ET, CTP:phosphoethanolamine cytidyltransferase; G3P, glycerol-3-phosphate; PEDS, plasmanyl-PE desaturase; PE-L, PE lower; PE-U, PE upper; plasmanyl-PC, 1-alkyl-2-acyl-glycerophosphocholine; plasmanyl-PE, 1-alkyl-2-acyl-glycerophosphoethanolamine; plasmenyl-PE; 1-alkenyl-2-acyl-glycerophosphoethanolamine (plasmalogen); PSD, PS decarboxylase.

¹To whom correspondence should be addressed.

e-mail: h-sugi@dokkyomed.ac.jp

^SThe online version of this article (available at <https://www.jlr.org>) contains a supplement.

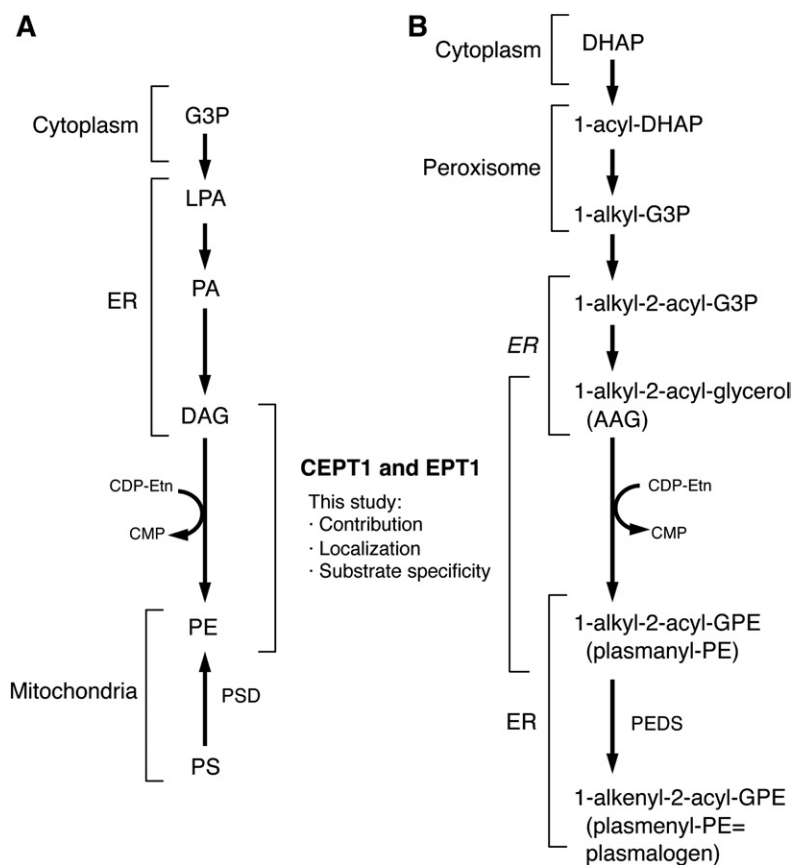


Fig. 1. Biosynthetic pathway and subcellular location for synthesis of EP in mammalian cells. The biosynthetic pathway of PE (A), plasmanyl-PE, and plasmenyl-PE (B) is shown. A detailed explanation is in the Introduction. This study reveals subcellular locations and contributions of EPT1 and CEPT1 to the biosynthesis of EP. GPE, glycerophosphoethanolamine; LPA, lysoPA.

decarboxylation pathway and the CDP-ethanolamine pathway generate different PE molecular species. In McA-RH7777 and Chinese hamster ovary K1 (CHO-K1) cells, the PS decarboxylation pathway is involved in the synthesis of PE molecular species mainly containing polyunsaturated fatty acids such as 18:0–20:4, 18:0–20:5, and 18:0–22:6. In contrast, the CDP-ethanolamine pathway preferentially synthesizes PE molecular species such as 16:0–18:2 and 18:1–18:2 (3).

The first step in the CDP-ethanolamine pathway is the phosphorylation of ethanolamine by ethanolamine kinase to produce ethanolamine phosphate. The second step is catalyzed by CTP:phosphoethanolamine cytidyltransferase (ET) encoded by *PCYT2*, which activates ethanolamine phosphate by interaction with CDP to produce CDP-ethanolamine. PE is finally synthesized by transferring phosphoethanolamine from CDP-ethanolamine to DAG, with the release of CMP by ethanolamine phosphotransferase. Two different ethanolamine phosphotransferases, such as choline/ethanolamine phosphotransferase 1 (CEPT1) (4) and ethanolamine phosphotransferase 1 (EPT1) (5), are involved in this final step.

The biosynthesis of ether-linked PE requires peroxisomes, in which 1-alkyl-dihydroxyacetone phosphate (DHAP) is synthesized by DHAP acyltransferase and alkyl-DHAP synthase (Fig. 1B). After reduction of 1-alkyl-DHAP to produce 1-alkyl-glycerol-3-phosphate (G3P) in peroxisomes, the intermediate is transferred to the ER and acylated to generate 1-alkyl-2-acyl-G3P, which is then dephosphorylated to produce AAG. For the synthesis of plasmenyl-PE, plasmanyl-PE is first synthesized from CDP-ethanolamine

and AAG by ethanolamine phosphotransferase, then the 1-alkyl group in plasmanyl-PE is desaturated to the 1-alkenyl group by plasmanyl-PE desaturase (PEDS), producing plasmenyl-PE (6). The *TMEM189* gene was recently identified as encoding PEDS (7, 8).

CEPT1 is the first ethanolamine phosphotransferase whose gene was identified and was believed to be solely responsible for catalyzing the final step of the CDP-ethanolamine pathway. CEPT1 is distributed in the ER and nuclear membranes of CHO-K1 cells (9). Both CDP-ethanolamine and CDP-choline are substrates for CEPT1 (4), although kinetic analysis demonstrated that CEPT1 prefers CDP-choline over CDP-ethanolamine as the phosphobase donor. In vitro enzymatic assays also revealed that CEPT1 prefers DAG 18:1–18:1 > DAG 16:1–16:1, 16:0–18:1, 16:0–22:6 as lipid acceptors.

Eight years after the molecular cloning of CEPT1, a gene encoding another ethanolamine phosphotransferase, EPT1, was identified by homology searches of the NCBI data bank with reference to the CDP-alcohol phosphatidyltransferase motif, a common motif conserved in phospholipid synthases (5). EPT1 (also called selenoprotein I) specifically transfers CDP-ethanolamine as the phosphobase donor (5). In humans, this enzyme is distributed primarily in brain, placenta, liver, and pancreas, followed by heart, skeletal muscle, lung, and kidney, although its cellular distribution remains unknown. We previously reported exon skipping in the *EPT1* gene in a patient suffering from a neurodegenerative disorder (10). The patient's skin fibroblasts had decreased levels of PE molecular species such as

38:6, 38:4, 40:6, 40:5 and 40:4 and, interestingly and more drastically, a decreased level of plasmenyl-PE. These results suggested that EPT1 plays an important role in the maintenance of plasmenyl-PE in humans. Another *EPT1* mutation was reported in patients with a similar neurodegenerative phenotype (11). However, the precise contribution of EPT1 and CEPT1 to the de novo biosynthesis of EP molecular species remains poorly characterized.

In the present study, we analyzed the intracellular distribution of EPT1 and CEPT1 and found that EPT1 is localized in the Golgi apparatus and CEPT1 is localized in the ER. We prepared *EPT1*-KO, *CEPT1*-KO, and double-KO (DKO) HEK293 cells and analyzed the de novo biosynthesis of EP molecular species in these cells using radio- and deuterium-labeled ethanolamine. These metabolic labeling experiments demonstrated that EPT1 preferentially biosynthesizes plasmenyl-PE and PE molecular species such as 36:1, 38:5, 38:4, 38:3, 40:6, 40:5, and 40:4, whereas CEPT1 is important for the biosynthesis of PE molecular species such as 32:2, 32:1, 34:2, and 34:1. An in vitro substrate specificity assay for determining lipid acceptors revealed that EPT1 catalyzes AAG 16–20:4 > DAG 18:0–20:4 > DAG 16:0–18:1 = AAG 16–18:1. In contrast, CEPT1 catalyzes DAG 16:0–18:1 much more preferentially compared with other lipid acceptors. These results suggest that EPT1 and CEPT1 are distributed in different organelles in cells and contribute to the synthesis of different types of EP molecular species.

MATERIALS AND METHODS

Cell culture and generation of *CEPT1*-KO, *EPT1*-KO, and double-KO HEK293 cells by genome editing using CRISPR-Cas9

HEK293 cells were cultured in DMEM (high glucose) with 10% FBS. Cells were maintained at 37°C in a humidified incubator containing 5% CO₂. To generate *CEPT1*-KO, *EPT1*-KO and *ET*-KO HEK293 cells using CRISPR-Cas9 technology, guide RNAs were designed as follows: *CEPT1* (sense, 5'-caccgTGAGTGGG-CATCGATCAACA-3'; antisense, 5'-aacTGTTGATCGATGCCCATCAc-3'), *EPT1* (sense, 5'-caccgAGTTTTTCGGGTCGTCATGGC-3'; antisense, 5'-aacGCCATGACGACCCGAAACTc-3'), and *ET* (sense, 5'-caccgTGTAAGCCCGCGATGATGTA-3'; antisense, 5'-aacTACATCATCGCGGCTTACAc-3'). Guide RNAs were cloned into the pSpCas9(BB)-2A-Puro (pX459) vector (Addgene, Cambridge, MA). Cells were transfected with these vectors using Lipofectamine 2000 transfection reagent (Thermo Fisher Scientific, Waltham, MA) according to the manufacturer's instructions. To establish the DKO cells, vectors containing both *EPT1* and *CEPT1* guide RNA were cotransfected into the HEK293 cells at the same time. Forty-eight hours after transfection, the cells were cultured in the presence of 1 µg/ml puromycin for 2 days, and then surviving cells were plated as single colonies in 96-well plates. Single clones were expanded and screened by measuring enzyme activity. To verify mutations, genomic DNA was isolated from the cells using Easy DNA extraction kit (Kaneka Corp., Tokyo, Japan), and the DNA fragments around the guide RNA target were amplified by PCR. The following primers were used: 5'-CCTCC-TTTTCTGGTCTGTTGATACTTAC-3'/5'-TATCTTTAGTTAA AATGACCCACGATCCC-3' for *CEPT1*; and 5'-AGCGC-

GGCTCTCCTACCTTCTCGGGCAGC-3'/5'-AAATAGGAAGGG AATCCCTCGCTCCATG-3' for *EPT1*. After being purified using a QIAquick gel extraction kit (Qiagen, Hilden, Germany), PCR products were cloned into T-vector pMD (Takara Bio Inc., Shiga, Japan). DNA sequences of several clones were determined using an ABI PRISM 377-XL DNA sequencer (Applied Biosystems, Foster City, CA) and a BigDye Terminator v1.1 cycle sequencing kit (Applied Biosystems).

Immunocytochemistry

EPT1 and *CEPT1* fused with a HA-tag at the C terminus were amplified by PCR and cloned into the pCAG vector (Wako Pure Chemical Industries, Osaka, Japan). Cells were grown on glass coverslips coated with 1% Cellmatrix (Nitta Gelatin, Osaka, Japan). Expression vectors were transfected into cells using Lipofectamine 2000. To label the ER, cells were cotransfected with pDsRed-ER vector encoding a red fluorescent protein fused with the ER retention sequence of calreticulin (Takara Bio Inc.). After 24 h, the cells were fixed with 4% paraformaldehyde in PBS for 15 min, washed with PBS, permeabilized with 0.1% Triton X-100 (w/v) for 10 min, and then blocked with 5% skim milk for 30 min. The cells were then incubated with anti-HA (Cell Signaling Technology, Danvers, MA), anti-GM130 (Sigma-Aldrich, St. Louis, MO), and anti-ERp72 (Cell Signaling Technology) antibodies overnight at 4°C, followed by washing and immunostaining with fluorescently labeled secondary antibodies conjugated with Alexa 488 or 594 (Thermo Fisher Scientific) for 1 h at room temperature. Nuclei were stained with DAPI. Samples were observed with a confocal microscope (LSM780; Zeiss, Oberkochen, Germany).

Expression of *CEPT1* and *EPT1* in DKO cells, and immunoblotting

The DKO cells were transfected with expression vectors containing HA-tagged *EPT1* or *CEPT1* using Lipofectamine 2000 and incubated for 24 h. Proteins were separated with SDS-PAGE, transferred to PVDF membranes (FluoroTrans, Pall Corp., Port Washington, NY) using a Trans-Blot SD semi-dry transfer blotter (Bio-Rad Laboratories, Hercules, CA), and then the membranes were incubated with 5% (w/v) skim milk in TBS for 1 h and washed three times with T-TBS (TBS containing 0.02% Tween 20). The membranes were then incubated with anti-HA tag antibody (Cell Signaling Technology) overnight at 4°C, washed three times with T-TBS, and then incubated with horseradish peroxidase-conjugated IgGs for 1 h at room temperature. The membranes were washed three times with T-TBS and stained with Clarity Western ECL substrate (Bio-Rad) according to the manufacturer's instructions and visualized using a ChemiDoc Touch imaging system (Bio-Rad).

BFA treatment, metabolic labeling of EPs with radiolabeled ethanolamine, and TLC analysis

For metabolic labeling of EPs with radiolabeled ethanolamine, cells were cultured in medium containing 0.2 µCi/ml of ¹⁴C-ethanolamine [1,2-¹⁴C] (American Radiolabeled Chemicals, St. Louis, MO) for 2 h. Cells were pretreated with brefeldin A (BFA) (Cayman, Ann Arbor, MI) at a concentration of 20 µg/ml for 2 h, and then cultured with ¹⁴C-ethanolamine in the presence of BFA for 4 h. Phospholipids were extracted from the cells using the Bligh and Dyer method (12). Radiolabeled phospholipids were applied to precoated silica gel 60 TLC plates (Merck, Darmstadt, Germany) and developed with chloroform-methanol-water (65:25:4, v/v/v). To separate plasmenyl-PE and PE, the TLC plates were exposed to HCl vapor for 3 min at room temperature before development to hydrolyze the 1-alkenyl group in plasmenyl-PE. The radioactivities of PE and the lyso-form of PE derived from plasmenyl-PE were

analyzed using a FLA-7000 imaging analyzer and quantified using ImageQuant TL version 8.1 (GE Healthcare UK Ltd., Amersham, UK).

Metabolic labeling of EPs with deuterium-labeled ethanolamine and quantification of phospholipids by LC-MS/MS

EPs were metabolically labeled with deuterium-labeled ethanolamine by culturing cells in medium containing 1 mM *d4*-ethanolamine (ethanol-1,1,2,2-*d4*-amine) (Cambridge Isotope Laboratories, Andover, MA) for 4 h. After washing twice with PBS, the cells were lysed in 20 mM Tris-HCl buffer (pH 8.0) and the amount of protein was measured using a BCA protein assay kit (Thermo Fisher Scientific). Phospholipids were extracted from cell lysate containing 300–400 μ g of protein using the Bligh and Dyer method in the presence of 1.5 nmol of internal standards (1,2-diheptadecanoyl PE and 1,2-dipentadecanoyl PC; Avanti Polar Lipids, Alabaster, AL). Lipids were analyzed by reverse-phase high-pressure LC using an L-column 2 ODS column (3 μ m, 2.0 \times 100 mm) (Chemicals Evaluation and Research Institute, Tokyo, Japan) coupled to a 5500 QTRAP mass spectrometer (Sciex Inc., Framingham, MA). A binary gradient consisting of solvent A (acetonitrile:methanol:water, 1:1:3, v/v/v, containing 5 mM ammonium acetate) and solvent B (2-propanol containing 5 mM ammonium acetate) was used. The gradient profile was as follows: 0–1 min, 95% A; 1–9 min, 5–95% B linear gradient; 9–13 min, 95% B. The flow rate was 0.2 ml/min, and the column temperature was 40°C. EP species were detected in multiple reaction monitoring mode by selecting the *m/z* of the phospholipid species at Q1 and the precursor ion of *m/z* 196 at Q3 in negative ion mode. For deuterium-labeled EPs, the precursor ion of *m/z* 200 at Q was monitored. To identify plasmenyl-PE containing 16:0, 18:0, and 18:1 at the *sn*-1 position, the precursor ions of *m/z* 364, 392, and 390 at Q3, respectively, were detected as described in (13). Lipids were quantified using MultiQuant version 2.0 (Sciex) and normalized against the internal standards and amount of protein.

In vitro enzymatic assay

Ethanolamine phosphotransferase activity was measured as described previously (5, 10). Briefly, cells were lysed in 20 mM Tris-HCl, pH 8.0, containing 5 μ g/ml each of leupeptin, pepstatin, and chymostatin in an ultrasonic bath sonicator for 10 s. The protein content was measured using a BCA protein assay kit. The reaction mixture (30 μ l) contained 50 mM Tris-HCl buffer, pH 8.0, 5 mM MnCl₂, 1 mM EGTA, 0.03% Tween 20 (w/v), cell lysate, 20 μ M CDP-ethanolamine [1,2-¹⁴C], and 1.5 mM DAG 18:1–18:1 (Sigma-Aldrich), DAG 16:0–18:1 (Avanti Polar Lipids), or DAG 18:0–20:4 (Cayman). AAG 16–18:1 and AAG 16–20:4 were prepared as follow. After incubation at 37°C for 15 min, the reaction was stopped by adding 300 μ l of chloroform-methanol (1:1, v/v), and then 110 μ l water was added. After centrifugation at 12,000 *g* for 5 min, the organic phase was applied to TLC plates and analyzed as described above.

Preparation of AAG

AAG was prepared by digesting plasmanyl-PC with phospholipase C (14). Briefly, 1 mg of 1-*O*-hexadecyl-2-oleoyl-*sn*-glycero-3-phosphocholine (plasmanyl-PC 16–18:1; Avanti Polar Lipids) or 1-*O*-hexadecyl-2-arachidonoyl-*sn*-glycero-3-phosphocholine (plasmanyl-PC 16–20:4; Cayman) was dissolved in 1 ml of 50 mM HEPES buffer, pH 7.5, containing 3 mM CaCl₂. Then, 0.3 mg of phospholipase C from *Clostridium perfringens* type I (Sigma-Aldrich) and 1.5 ml of diethyl ether were added. After incubation at 37°C for 1 h with gentle shaking, the ether phase containing AAG was recovered.

Statistical analysis

Quantitative data are presented as mean \pm SD. Statistical significance was assessed using the Student's *t*-test or one-way ANOVA with Dunnett's post hoc test. A *P* value of <0.05 was considered statistically significant.

RESULTS

EPT1 is distributed in the Golgi apparatus whereas CEPT1 is localized in the ER

In mammalian cells, CEPT1 was reported to be distributed in the ER and nuclear envelope (9). In contrast, there have been no reports regarding the intracellular localization of EPT1, except in the parasite *Trypanosoma brucei*, in which the enzyme is exclusively found in the perinuclear ER (15). To compare the intracellular distribution of CEPT1 and EPT1 in mammalian cells, the enzymes were fused with a HA-tag at the C terminus and overexpressed in HEK293 cells, stained with anti-HA-tag antibody, followed by its second antibody. As shown in Fig. 2A, the green signal of CEPT1 was colocalized with the red signal of ERp72, indicating that the enzyme is distributed in the ER. In contrast, the signal of EPT1 was merged with GM130, indicating that the enzyme is localized in the Golgi apparatus (Fig. 2B). These results suggest that the intracellular sites for the production of EP by EPT1 or CEPT1 are different.

The de novo biosynthesis of PE-U, PE-L, and plasmenyl-PE from ¹⁴C-ethanolamine in EPT1-KO, CEPT1-KO, and DKO cells

We evaluated the contributions of EPT1 and CEPT1 to EP molecular species by preparing *EPT1*-KO, *CEPT1*-KO,

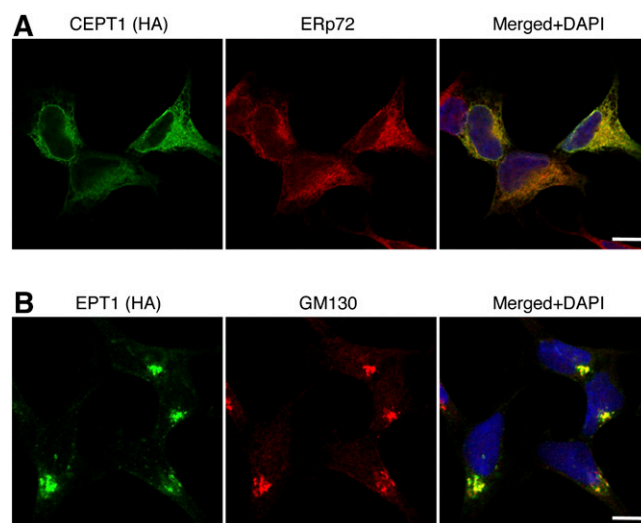


Fig. 2. Immunocytochemistry of EPT1 and CEPT1 in HEK293 cells. HEK293 cells were transfected with the expression vector for CEPT1 (A) or EPT1 (B) tagged with HA at the C terminus. After fixation, the cells were permeabilized with 0.1% Triton X-100 (w/v), then immunostained with anti-HA antibody, followed by anti-mouse IgG Alexa488 (green). The ER and Golgi apparatus were stained with anti-ERp72 and GM130 antibodies, respectively, followed by anti-rabbit IgG Alexa594 (red). Nuclei were stained with DAPI (blue). Scale bars indicate 10 μ m.

and DKO cells using the CRISPR-Cas9 system (supplemental Fig. S1). In vitro phosphotransferase activity was assayed using cell lysates as an enzyme source, radiolabeled CDP-ethanolamine as a phosphoethanolamine donor, and DAG 18:1–18:1 as a lipid acceptor. Synthesized radioactive PE was separated by TLC (Fig. 3A) and the radioactivity of each lipid band was quantified (Fig. 3B). The results showed that the phosphotransferase activities in *EPT1*-KO and *CEPT1*-KO cell lysates were reduced by about 90% and 25% of that of WT cells, respectively. These results suggest that the contribution of *EPT1* in PE biosynthesis is much higher than that of *CEPT1*. No radiolabeled PE band was observed in the DKO cells, suggesting that the total activity of phosphotransferase in HEK293 cells is clearly derived from both *EPT1* and *CEPT1*.

The de novo biosynthesis of EP was analyzed by metabolic labeling with radiolabeled ethanolamine. We evaluated the contribution of the CDP-ethanolamine pathway for the biosynthesis of EP by establishing *ET*-KO cells using the CRISPR-Cas9 system. *ET* is an enzyme responsible for the biosynthesis of CDP-ethanolamine. WT, *CEPT1*-KO, *EPT1*-KO, DKO, and *ET*-KO cells were cultured in the presence of 14 C-ethanolamine. The lipid phases were extracted from the cells and spotted onto TLC plates. Plasmenyl-PE was separated from PE by exposing the TLC plate to HCl vapor to hydrolyze the alkenyl-group in plasmenyl-PE before development, resulting in formation of the lyso-form of the lipid (16). As shown in Fig. 3C, the degraded form of plasmenyl-PE due to HCl (the lyso-form) appeared under the PE band. Interestingly, PE bands with different Rf values, termed PE upper (PE-U) and PE lower (PE-L), were detected in the *CEPT1*-KO and *EPT1*-KO cells, respectively.

The *CEPT1*-KO cells preferentially generated PE-U, whereas *EPT1*-KO cells generated PE-L (Fig. 3D). These results suggest that *EPT1* and *CEPT1* contribute to the biosynthesis of different PE molecular species. The lyso-form of degraded plasmenyl-PE was not observed in the *EPT1*-KO and DKO cells (Fig. 3C, E), suggesting that the production of plasmenyl-PE in HEK293 cells is mainly dependent on *EPT1*. Both PE and the lyso-form of degraded plasmenyl-PE were absent in the DKO and *ET*-KO cells, suggesting that the CDP-ethanolamine pathway was completely deleted in these cells.

Confirmation experiments for the synthesis of PE-U, PE-L, and plasmenyl-PE in *EPT1*- or *CEPT1*-reintroduced DKO cells

The results of metabolic labeling with radiolabeled ethanolamine suggest that *EPT1* preferentially synthesizes PE-U and plasmenyl-PE, whereas *CEPT1* preferentially produces PE-L (Fig. 3C). To clarify these results, expression vectors of *EPT1* or *CEPT1* fused with a HA-tag at the C terminus were reintroduced into the DKO cells. As shown Fig. 4A, 33 kDa protein bands were stained by anti HA-tag antibody in DKO cells reintroduced with either *CEPT1* or *EPT1*. For reasons presently unknown, the observed molecular mass of 33 kDa was smaller than the estimated molecular mass of *CEPT1* (46.5 kDa) or *EPT1* (45.0 kDa). The cells were then incubated with 14 C-ethanolamine, and the phospholipids were extracted and analyzed by TLC. As shown in Fig. 4B, PE-L was present in the *CEPT1*-reintroduced DKO cells. PE-U and plasmenyl-PE were also clearly synthesized in the *EPT1*-reintroduced DKO cells. The radioactivities of the lipid bands were calculated, as shown in Fig. 4C. The production of plasmenyl-PE by *EPT1* was significantly higher

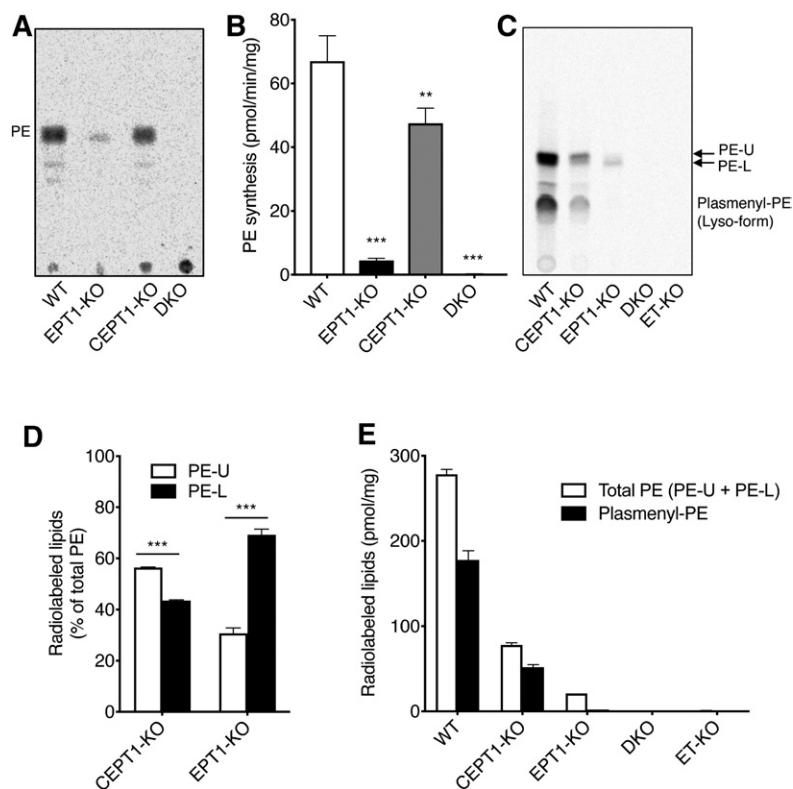


Fig. 3. In vitro enzymatic activity and the de novo biosynthesis of EPs from radiolabeled ethanolamine in *EPT1*- and/or *CEPT1*-deficient HEK293 cells. A: Ethanolamine phosphotransferase activity in cell lysates from WT, *EPT1*-KO, *CEPT1*-KO, and DKO HEK293 cells. Enzymatic activity was measured using radiolabeled CDP-ethanolamine and DAG 18:1–18:1 as substrates at 37°C for 15 min. After extraction, radioactive PE was analyzed by TLC (A) and quantified using ImageQuant TL version 8.1 (B). Values shown are mean \pm SD from three independent assays. ** $P < 0.01$ and *** $P < 0.001$ as compared with WT cells, as determined using one-way ANOVA with Dunnett's post hoc test. C: Metabolic labeling of EPs with radiolabeled ethanolamine. Cells were incubated with 14 C-ethanolamine for 2 h. After extraction, lipids were treated with HCl vapor to degrade plasmenyl-PE to the lyso-form of the lipid. Radioactive lipids were analyzed by TLC. D: Percentage of PE-U or PE-L in the total PE (PE-U + PE-L) in C was calculated. Values shown are mean \pm SD from three independent culture dishes. *** $P < 0.001$ as determined using Student's *t*-test. E: Quantification of total PE (PE-U + PE-L) and plasmenyl-PE in C. The amount of radiolabeled lipids was normalized by the amount of total cellular protein.

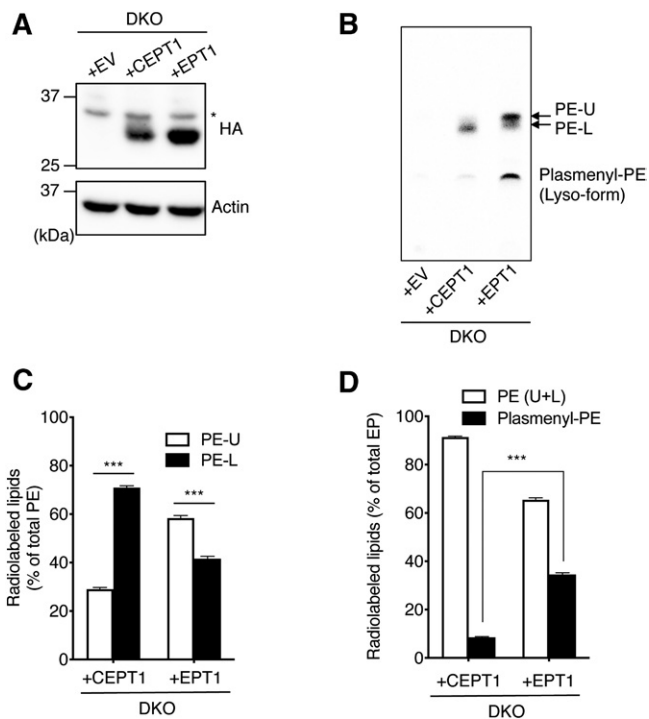


Fig. 4. The de novo biosynthesis of EPs from radiolabeled ethanolamine in DKO HEK293 cells containing reintroduced EPT1 or CEPT1. **A:** DKO cells were transfected with empty vector (EV) or with vector containing CEPT1 or EPT1 fused with a HA-tag at the C terminus. After 24 h, the cell lysates were separated by SDS-PAGE and HA-tagged proteins were analyzed by immunoblotting using anti-HA antibody. Actin was used as a protein loading control. The asterisk indicates a nonspecific signal. **B:** Metabolic labeling of EPs with radiolabeled ethanolamine. DKO cells transfected with EV or with vector containing CEPT1 or EPT1 were incubated with ^{14}C -ethanolamine for 2 h. After extraction, radioactive lipids were analyzed by TLC after HCl treatment to convert plasmalogen-PE into the lyso-form. **C:** Relative amount of PE-U or PE-L in total PE (PE-U + PE-L) in B was calculated. **D:** Relative amount of total PE (PE-U + PE-L) or plasmalogen-PE in total EP (PE + plasmalogen-PE) in B was calculated. Values shown are mean \pm SD from three independent culture dishes. *** $P < 0.001$ as determined by Student's *t*-test.

than that by CEPT1 (Fig. 4D). These results support our findings that CEPT1 and EPT1 preferentially de novo biosynthesize PE-L and PE-U/plasmalogen-PE, respectively.

Metabolic labeling of EP with *d4*-ethanolamine and quantification of PE and plasmalogen-PE molecular species by LC-MS/MS

The mobility of a phospholipid on a silica TLC plate is usually proportional to its hydrophobicity, suggesting that PE-L and PE-U contain shorter and longer fatty acids, respectively. To confirm this, we analyzed in detail the EP molecular species after metabolic labeling with *d4*-ethanolamine. The deuterium-labeled EPs could be distinguished from unlabeled endogenous lipids by LC-MS/MS because of a 4 Da mass difference. After *EPT1*-KO and *CEPT1*-KO cells were incubated with *d4*-ethanolamine, the labeled PE and plasmalogen-PE molecular species were analyzed by LC-MS/MS. As shown in Fig. 5A, the *EPT1*-KO cells significantly produced PE molecular species, such as 32:2, 32:1,

34:2, and 34:1, compared with the *CEPT1*-KO cells. In contrast, the *CEPT1*-KO cells significantly produced PE molecular species with longer fatty acids, such as 36:1, 38:5, 38:4, 38:3, 40:6, 40:5, and 40:4, compared with the *EPT1*-KO cells.

We verified these results by repeating the same experiments with *d4*-ethanolamine using DKO cells reintroduced with either EPT1 or CEPT1. As shown in Fig. 5B, the CEPT1-reintroduced DKO cells preferentially synthesized PE molecular species containing 32:2, 32:1, 34:2, and 34:1 compared with EPT1-reintroduced DKO cells. On the other hand, EPT1-reintroduced DKO cells significantly produced PE molecular species 36:1, 38:6, 38:5, 38:4, and 40:6 compared with CEPT1-reintroduced cells. These results support the possibility that EPT1 and CEPT1 preferentially produce PE molecular species containing longer and shorter fatty acids, respectively.

Next, we compared the deuterium-labeled plasmalogen-PE molecular species. As shown in Fig. 5C and D, the *CEPT1*-KO and EPT1-reintroduced DKO cells contained much higher amounts of plasmalogen-PE molecular species than *EPT1*-KO and CEPT1-reintroduced DKO cells. Again, these results strongly support our finding that the biosynthesis of plasmalogen-PE is largely dependent on EPT1.

The endogenous amounts of PE, plasmalogen-PE, PC, and plasmalogen-PC molecular species

We compared the endogenous amounts of PE molecular species in WT, *CEPT1*-KO, *EPT1*-KO, and DKO cells. As shown in Fig. 6A, there was no significant difference between WT, *CEPT1*-KO, and *EPT1*-KO cells, except for PE 36:1. In DKO cells, the levels of PE molecular species, such as 34:2, 34:1, 36:2, and 36:1, were significantly decreased compared with WT. Unexpectedly, the content of PE 38:4 and PE 38:5 in DKO cells was significantly increased compared with WT cells. These results suggest that deletion of either EPT1 or CEPT1 has no significant effect on the endogenous levels of PE molecular species. We then quantified the endogenous amount of plasmalogen-PE molecular species. As shown in Fig. 6B, there was no significant change between WT and *CEPT1*-KO cells. However, the levels of almost all plasmalogen-PE molecular species were reduced in *EPT1*-KO and DKO cells compared with WT cells, suggesting that EPT1 is much more important for the retention of plasmalogen-PE than is CEPT1.

The endogenous amounts of PC and plasmalogen-PC molecular species were also compared between WT, *CEPT1*-KO, *EPT1*-KO, and DKO cells. There was no difference in the level of PC (supplemental Fig. S2A), whereas significant increases in the levels of plasmalogen-PC molecular species were observed in the *EPT1*-KO and DKO cells (supplemental Fig. S2B). These results indicate that EPT1 is also involved in regulation of the plasmalogen-PC content.

Effect of BFA on the de novo biosynthesis of EP molecular species

As shown in Fig. 2, EPT1 and CEPT1 are localized in the Golgi apparatus and the ER, respectively. To verify the possibility that the preferential synthesis of PE-U and

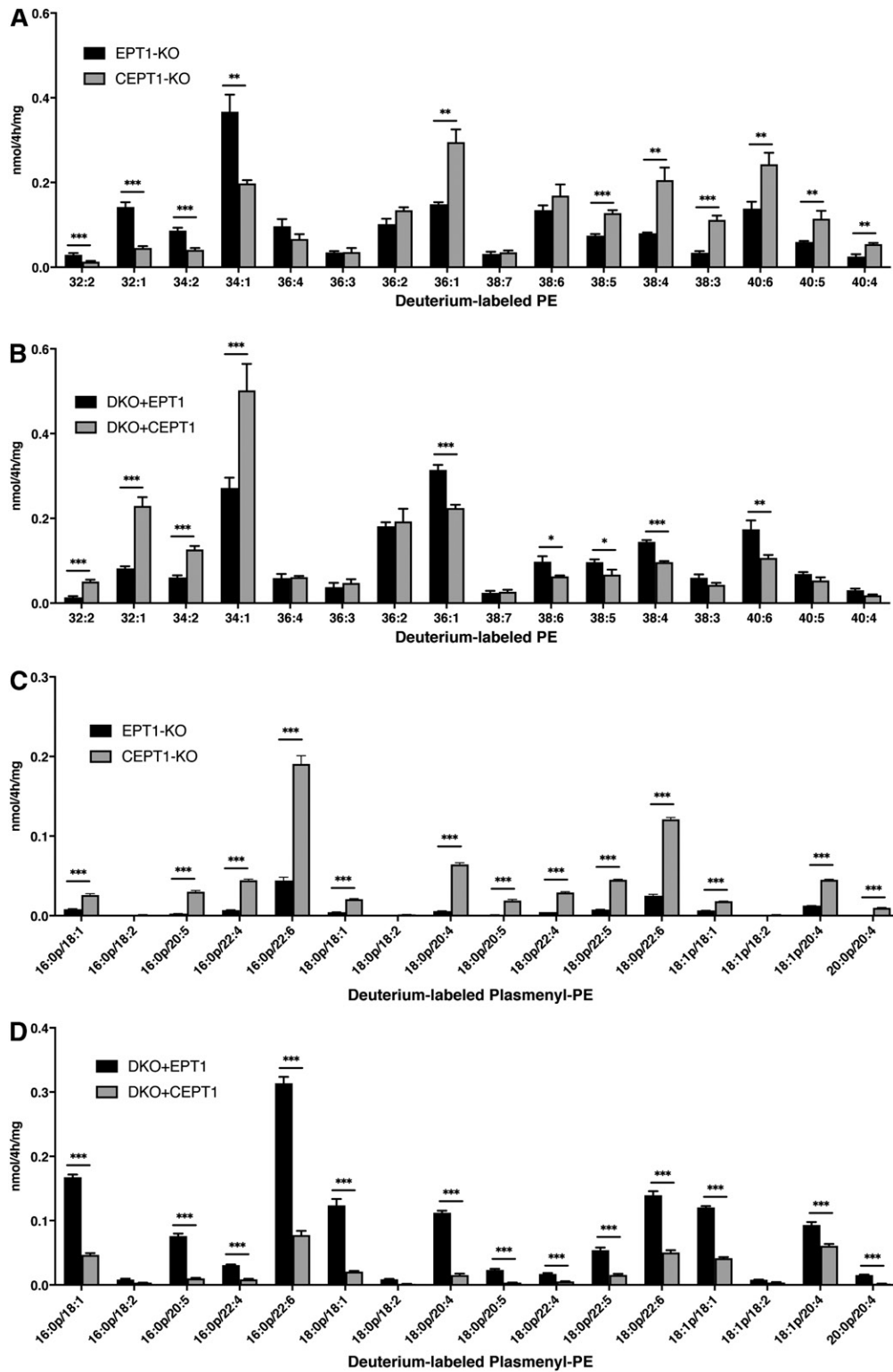


Fig. 5. The de novo biosynthesis of EPs from deuterium-labeled ethanolamine and quantification by LC-MS/MS. *EPT1*-KO or *CEPT1*-KO (A, C) DKO cells expressing *EPT1* or *CEPT1* (B, D) were incubated with deuterium-labeled ethanolamine for 4 h. After extraction, the levels of deuterium-labeled PE (A, B) and plasmeyl-PE (C, D) molecular species were quantified using LC-MS/MS. The lipid amount was normalized by the amount of total cellular proteins. * $P < 0.05$, ** $P < 0.01$, and *** $P < 0.001$ as determined by Student's *t*-test.

plasmeyl-PE by *EPT1* and PE-L by *CEPT1* is dependent on the difference in their subcellular localization, we assessed the effect of BFA, which promotes fusion of the Golgi membrane with the ER. After transfection with HA-tagged

CEPT1 or *EPT1*, DKO cells were treated with BFA and the intracellular distribution of these enzymes was analyzed by immunofluorescence. As shown in supplemental Fig. S3A, the location of GM130 was dispersed after BFA treatment

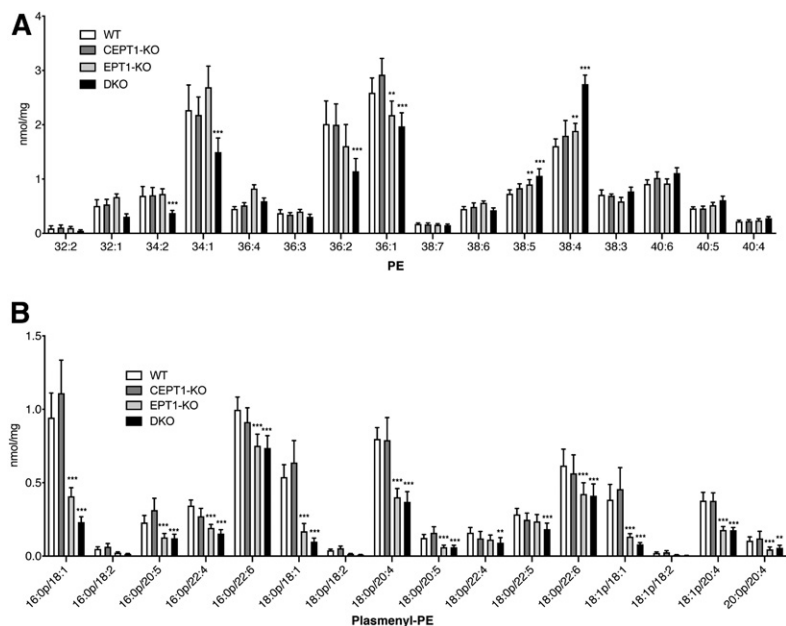


Fig. 6. Amount of endogenous PE and plasmeyl-PE molecular species in WT, *EPT1*-KO, *CEPT1*-KO, and DKO HEK293 cells. The endogenous levels of PE (A) and plasmeyl-PE (B) molecular species were quantified using LC-MS/MS. Data are mean \pm SD from nine independent culture dishes. * $P < 0.05$, ** $P < 0.01$, and *** $P < 0.001$ as compared with WT cells determined using one-way ANOVA with Dunnett's post hoc test. Lipid levels were normalized by the amount of total cellular protein.

as described in (17). *EPT1* was colocalized with the ER-targeted fluorescent protein DsRed after BFA treatment, indicating that the localization of *EPT1* was changed from the Golgi apparatus to the BFA-treated ER (supplemental Fig. S3B). In contrast, *CEPT1* was consistently distributed in the ER before and after BFA treatment (supplemental Fig. S3C). EP was then metabolically labeled with radiolabeled ethanolamine in the presence of BFA. As shown in **Fig. 7A**, BFA treatment did not induce significant changes in the level of PE-L following reintroduction of *CEPT1* in DKO cells, or in PE-U and plasmeyl-PE following reintroduction of *EPT1* in DKO cells. Similar results were obtained with *CEPT1*-KO and *EPT1*-KO cells metabolically labeled with 14 C-ethanolamine in the presence of BFA (Fig. 7B). The influence of BFA on the de novo biosynthesis of PE molecular species was also examined by metabolic labeling with *d4*-ethanolamine. BFA caused no significant changes in the level of metabolically labeled PE molecular species in *EPT1*-reintroduced DKO (Fig. 7C) and *CEPT1*-KO cells (Fig. 7D) or in plasmeyl-PE molecular species (supplemental Fig. S4A and B, respectively). These results suggest that subcellular localization is not important for the preferential synthesis of PE and plasmeyl-PE molecular species by *EPT1* and *CEPT1*.

In vitro lipid acceptor specificity of *EPT1* and *CEPT1*

We confirmed that the preferential synthesis of EP molecular species is dependent on enzymatic specificity toward lipid acceptors by assessing ethanolamine phosphotransferase activities toward two DAG molecular species. DAG 16:0–18:1 and DAG 18:0–20:4 were used because they are representative DAG molecular species of PE-L and PE-U, respectively (Fig. 5A, B). We could not obtain sufficient active purified enzyme for this assay after protein solubilization and affinity chromatography purification (supplemental Fig. S5) and thus used cell lysates from DKO cells expressing *EPT1* or *CEPT1* as enzyme solutions. We compared the specificity by calculating the relative activity to-

ward DAG 18:0–20:4 and DAG 16:0–18:1. As shown in **Fig. 8A** and D, *EPT1* slightly but significantly preferred DAG 18:0–20:4 compared with DAG 16:0–18:1 as a lipid acceptor. In contrast, *CEPT1* preferred DAG 16:0–18:1 (2-fold higher) as a lipid acceptor compared with DAG 18:0–20:4 (Fig. 8E). These results clearly support our previous findings that *EPT1* preferentially produces PE-U while *CEPT1* produces PE-L.

We attempted to determine the specificity of *EPT1* and *CEPT1* toward AAG. AAG is not commercially available and thus AAG 16–18:1 and AAG 16–20:4 were prepared by digesting plasmeyl-PC 16–18:1 and plasmeyl-PC 16–20:4, respectively, using phospholipase C. To compare each result, we calculated the relative activity toward AAG 16–18:1 and AAG 16–20:4 compared with DAG 16:0–18:1. As shown in Fig. 8B–D, the preference of *EPT1* followed the order AAG 16–20:4 > DAG 18:0–20:4 > DAG 16:0–18:1 = AAG 16–18:1. In contrast, *CEPT1* preferentially used DAG 16:0–18:1 over other acceptors. Taken together, these results suggest that the preferential synthesis of EP molecular species by *EPT1* and *CEPT1* is dependent on differences in enzymatic specificity toward lipid acceptors.

DISCUSSION

The final step of EP generation via the CDP-ethanolamine pathway is catalyzed by *EPT1* and *CEPT1* but differences in the EP molecular species synthesized by each enzyme remain poorly characterized. In this study, metabolic labeling experiments with isotope-labeled ethanolamine clearly demonstrated for the first time that *EPT1* is distributed in the Golgi apparatus and preferentially produces PE-U and plasmeyl-PE, while *CEPT1* is distributed in the ER and preferentially synthesizes PE-L. A schematic diagram summarizing the main conclusion of this study is shown in supplemental Fig. S6. There was no evidential decreased change in the endogenous amounts of PE

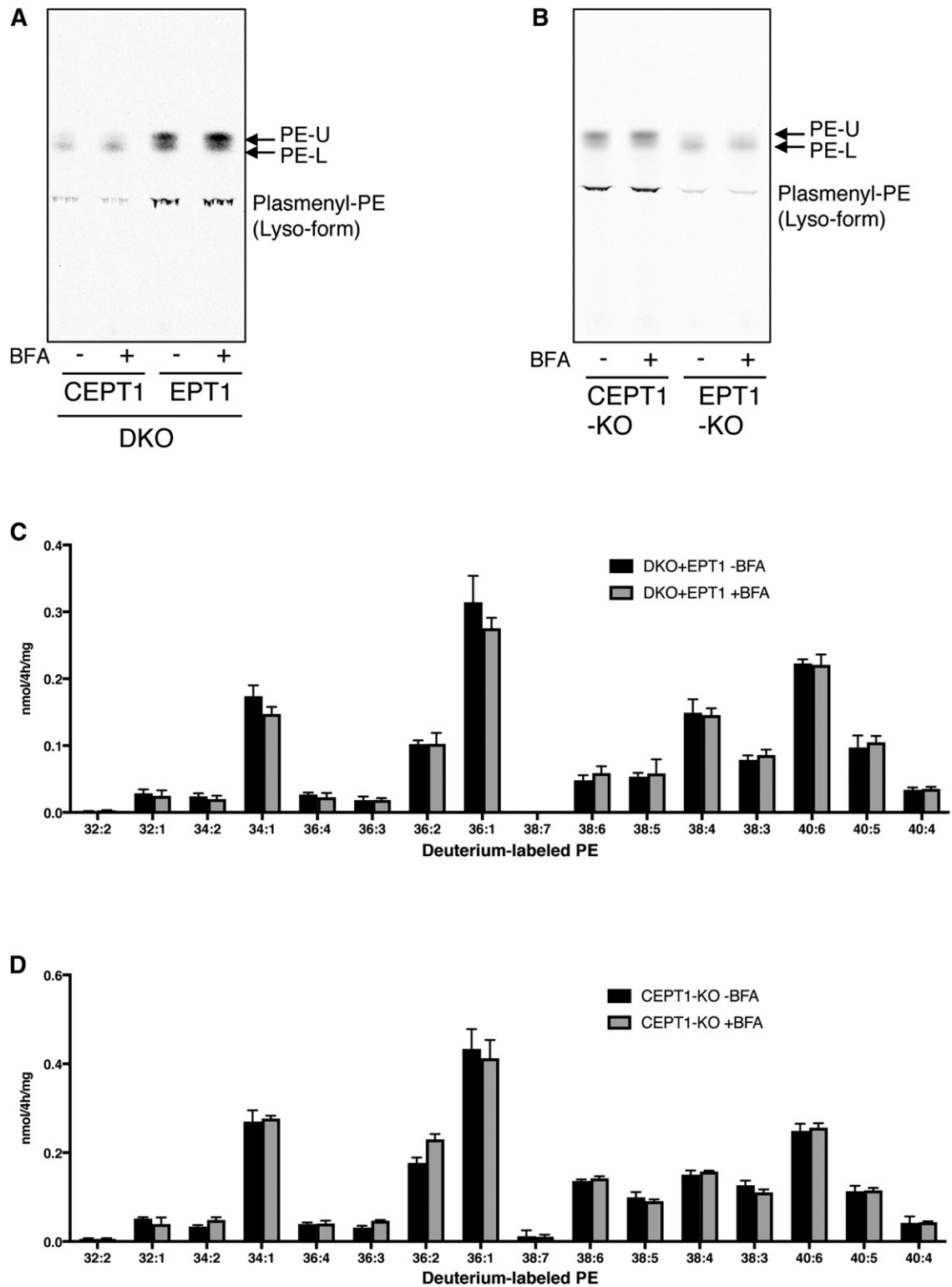


Fig. 7. Effect of BFA treatment on the de novo biosynthesis of EP molecular species in EPT1- or CEPT1-deficient HEK293 cells. A, B: Metabolic labeling of EPs with radiolabeled ethanolamine in the presence of BFA. After pretreatment with or without BFA for 2 h, DKO cells with reintroduced CEPT1 or EPT1 (A) or *CEPT1*- or *EPT1*-KO cells (B) were incubated with ^{14}C -ethanolamine. After extraction, radioactive lipids were analyzed by TLC. C, D: Metabolic labeling of EPs with deuterium-labeled ethanolamine with or without BFA. DKO cells expressing EPT1 (C) or *CEPT1*-KO cells (D) were incubated with d_4 -labeled ethanolamine with or without BFA for 4 h. After extraction, the level of deuterium-labeled PE molecular species was quantified using LC-MS/MS. The lipid level was normalized by the amount of total cellular protein.

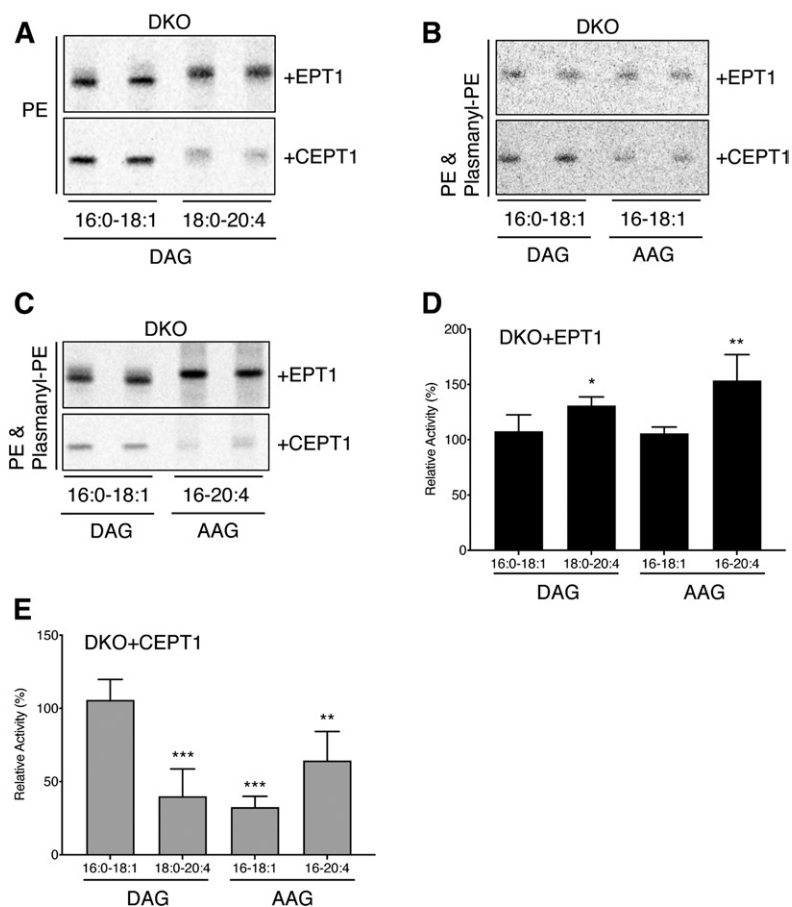


Fig. 8. In vitro enzymatic specificities toward several lipid acceptors of EPT1 and CEPT1. Ethanolamine phosphotransferase activities in cell lysates from DKO cells expressing EPT1 or CEPT1 were measured using radiolabeled CDP-ethanolamine and DAG 18:0-20:4 (A), AAG 16-18:1 (B), and AAG 16-20:4 (C) as substrates for 15 min at 37°C. For comparison, enzymatic activity for DAG 16:0-18:1 was measured in the same assay. D, E: Relative activity for each lipid acceptor compared with DAG 16:0-18:1 was calculated. Data are mean \pm SD from three independent assays. * $P < 0.05$, ** $P < 0.01$, and *** $P < 0.001$ as compared with DAG 16:0-18:1 using one-way ANOVA with Dunnett's post hoc test.

molecular species between WT, *CEPT1*-KO, and *EPT1*-KO cells (Fig. 6A), likely because the levels of PE are maintained by residual CEPT1 or EPT1, and by another PE-generating enzyme, such as PSD, and by PE remodeling enzymes. Significant decreases in PE molecular species, such as 34:2, 34:1, 36:2, and 36:1, were observed in DKO cells, suggesting that the CDP-ethanolamine pathway is critical for maintaining these PE molecular species. Interestingly, PE 38:4 and PE 38:5 were significantly increased in DKO cells compared with WT cells, for reasons currently unknown. PSD preferentially produces PE molecular species with polyunsaturated fatty acids, including PE 18:0-20:4 (3). Therefore, we speculate that the PSD pathway is activated and generates these PE molecular species to compensate for the loss of PE produced by the CDP-ethanolamine pathway.


We previously found that the level of plasmanyl-PE is significantly reduced in skin fibroblasts isolated from a patient with exon skipping in the *EPT1* gene (10). In the present study, we demonstrated that EPT1, but not CEPT1, is responsible for the maintenance of plasmanyl-PE (Fig. 6B). Although CEPT1 can synthesize plasmanyl-PE in vitro (Fig. 8), its enzymatic activity is likely insufficient for the biosynthesis of plasmanyl-PE in cells. We suggest two reasons why EPT1 makes a higher contribution than CEPT1 to the retention of plasmanyl-PE in cells. First, EPT1 has higher enzymatic activity than CEPT1 in cells (Fig. 3), and second, there is a difference in enzymatic specificity toward lipid acceptors, i.e., EPT1 greatly prefers AAG compared with CEPT1 (Fig. 8). The molecular mechanism underlying the

different affinities of EPT1 and CEPT1 toward their lipid acceptors and phosphobase donors remains unknown and will require studies using the crystal structure of these enzymes.

The endogenous plasmanyl-PE level was not completely abolished in *EPT1*-KO and DKO cells (Fig. 6B), although the synthesis of plasmanyl-PE from isotopic ethanolamine was dramatically reduced (Figs. 3C, 4B). These results suggest the presence of a pathway other than the CDP-ethanolamine pathway for the synthesis of plasmanyl-PE and plasmanyl-PE. Previous studies have demonstrated that serine can be incorporated into both the head group of PS and the head group of both plasmanyl-PE and plasmanyl-PE (18-20). In addition, there are several reports confirming the presence of plasmanyl-PS in lung (21), lens (22), macrophages (23), retina, and optic nerve (24). Thus, the PSD pathway may compensate for loss of the CDP-ethanolamine pathway. Further study is necessary to understand how the PSD pathway, or unknown pathways, synthesizes plasmanyl-PE. We previously found increased levels of plasmanyl-PC in patient cells with truncated EPT1 (10) and in *EPT1*-KO and DKO cells (supplemental Fig. S2B), possibly because the loss of plasmanyl-PE synthesis causes a surplus of AAG. CEPT1 and CPT in *EPT1*-KO cells, or CPT in the DKO cells, likely utilize excess AAG to generate plasmanyl-PC.

As shown here, EPT1 is distributed in the Golgi apparatus, and therefore plasmanyl-PE, a precursor for plasmanyl-PE, is likely pooled in the Golgi apparatus after synthesis.

Plasmanyl-PE is then desaturated and converted to plasmenyl-PE by the action of PEDS encoded by *TMEM189*. Interestingly, immunofluorescence staining demonstrated that *TMEM189* is localized in the ER (7, 8). These results suggest that plasmanyl-PE pooled in the Golgi may be transferred to the ER for desaturation by *TMEM189*, and then catalyzed to plasmenyl-PE. Recent studies show that the inter-organelle trafficking of lipids is mediated by various types of lipid transfer proteins at membrane contact sites (25). Plasmanyl-PE is therefore likely transferred between organelles by similar machinery.

In summary, this study demonstrated that EPT1 and CEPT1, the final enzymes for the synthesis of EP in the CDP-ethanolamine pathway, are distributed in the Golgi apparatus and ER, respectively. EPT1 mainly contributes to the biosynthesis of plasmenyl-PE and PE molecular species containing longer fatty acids, such as 36:1, 38:5, 38:4, 38:3, 40:6, and 40:5, and CEPT1 preferentially generates PE containing shorter fatty acids, such as 32:2, 32:1, 34:2, and 34:1. 

The authors would like to thank Dr. Takashi Namatame of the Clinical Research Center for DNA sequencing, Dokkyo Medical University.

REFERENCES

- Vance, J. E. 2015. Phospholipid synthesis and transport in mammalian cells. *Traffic*. **16**: 1–18.
- Vance, J. E. 2018. Historical perspective: phosphatidylserine and phosphatidylethanolamine from the 1800s to the present. *J. Lipid Res.* **59**: 923–944.
- Bleijerveld, O. B., J. F. Brouwers, A. B. Vaandrager, J. B. Helms, and M. Houweling. 2007. The CDP-ethanolamine pathway and phosphatidylserine decarboxylation generate different phosphatidylethanolamine molecular species. *J. Biol. Chem.* **282**: 28362–28372.
- Henneberry, A. L., and C. R. McMaster. 1999. Cloning and expression of a human choline/ethanolaminephosphotransferase: synthesis of phosphatidylcholine and phosphatidylethanolamine. *Biochem. J.* **339**: 291–298.
- Horibata, Y., and Y. Hirabayashi. 2007. Identification and characterization of human ethanolaminephosphotransferase1. *J. Lipid Res.* **48**: 503–508.
- Wykle, R. L., M. L. Blank, B. Malone, and F. Snyder. 1972. Evidence for a mixed function oxidase in the biosynthesis of ethanolamine plasmalogens from 1-alkyl-2-acyl-sn-glycero-3-phosphorylethanolamine. *J. Biol. Chem.* **247**: 5442–5447.
- Gallego-García, A., A. J. Monera-Girona, E. Pajares-Martinez, E. Bastida-Martinez, R. Perez-Castano, A. A. Iniesta, M. Fontes, S. Padmanabhan, and M. Elias-Arnanz. 2019. A bacterial light response reveals an orphan desaturase for human plasmalogen synthesis. *Science*. **366**: 128–132.
- Werner, E. R., M. A. Keller, S. Sailer, K. Lackner, J. Koch, M. Hermann, S. Coassin, G. Golderer, G. Werner-Felmayer, R. A. Zoeller, et al. 2020. The *TMEM189* gene encodes plasmanylethanolamine desaturase which introduces the characteristic vinyl ether double bond into plasmalogens. *Proc. Natl. Acad. Sci. USA*. **117**: 7792–7798.
- Henneberry, A. L., M. M. Wright, and C. R. McMaster. 2002. The major sites of cellular phospholipid synthesis and molecular determinants of fatty acid and lipid head group specificity. *Mol. Biol. Cell*. **13**: 3148–3161.
- Horibata, Y., O. Elpeleg, A. Eran, Y. Hirabayashi, D. Savitzki, G. Tal, H. Mandel, and H. Sugimoto. 2018. EPT1 (selenoprotein I) is critical for the neural development and maintenance of plasmalogen in humans. *J. Lipid Res.* **59**: 1015–1026.
- Ahmed, M. Y., A. Al-Khayat, F. Al-Murshedi, A. Al-Futaisi, B. A. Chioza, J. Pedro Fernandez-Murray, J. E. Self, C. G. Salter, G. V. Harlalka, L. E. Rawlins, et al. 2017. A mutation of EPT1 (SELEN0V) underlies a new disorder of Kennedy pathway phospholipid biosynthesis. *Brain*. **140**: 547–554.
- Bligh, E. G., and W. J. Dyer. 1959. A rapid method of total lipid extraction and purification. *Can. J. Biochem. Physiol.* **37**: 911–917.
- Zemski Berry, K. A., and R. C. Murphy. 2004. Electrospray ionization tandem mass spectrometry of glycerophosphoethanolamine plasmalogen phospholipids. *J. Am. Soc. Mass Spectrom.* **15**: 1499–1508.
- Takahashi, T., T. Sugahara, and A. Ohsaka. 1981. Phospholipase C from *Clostridium perfringens*. *Methods Enzymol.* **71**: 710–725.
- Farine, L., M. Niemann, A. Schneider, and P. Butikofer. 2015. Phosphatidylethanolamine and phosphatidylcholine biosynthesis by the Kennedy pathway occurs at different sites in *Trypanosoma brucei*. *Sci. Rep.* **5**: 16787.
- Frosolono, M. F., and M. M. Rapport. 1969. Reactivity of plasmalogens: kinetics of acid-catalyzed hydrolysis. *J. Lipid Res.* **10**: 504–506.
- Nakamura, N., C. Rabouille, R. Watson, T. Nilsson, N. Hui, P. Slusarewicz, T. E. Kreis, and G. Warren. 1995. Characterization of a cis-Golgi matrix protein, GM130. *J. Cell Biol.* **131**: 1715–1726.
- Xu, Z., D. M. Byers, F. B. Palmer, and H. W. Cook. 1994. Serine and ethanolamine incorporation into different plasmalogen pools: subcellular analyses of phosphoglyceride synthesis in cultured glioma cells. *Neurochem. Res.* **19**: 769–775.
- Yavin, E., and B. P. Zeigler. 1977. Regulation of phospholipid metabolism in differentiating cells from rat brain cerebral hemispheres in culture. Serine incorporation into serine phosphoglycerides: base exchange and decarboxylation patterns. *J. Biol. Chem.* **252**: 260–267.
- Yorek, M. A., R. T. Rosario, D. T. Dudley, and A. A. Spector. 1985. The utilization of ethanolamine and serine for ethanolamine phosphoglyceride synthesis by human Y79 retinoblastoma cells. *J. Biol. Chem.* **260**: 2930–2936.
- Kaneshiro, E. S., Z. Guo, D. Sul, K. A. Kallam, K. Jayasimhulu, and D. H. Beach. 1998. Characterizations of *Pneumocystis carinii* and rat lung lipids: glyceryl ethers and fatty alcohols. *J. Lipid Res.* **39**: 1907–1917.
- Deeley, J. M., M. C. Thomas, R. J. Truscott, T. W. Mitchell, and S. J. Blanksby. 2009. Identification of abundant alkyl ether glycerophospholipids in the human lens by tandem mass spectrometry techniques. *Anal. Chem.* **81**: 1920–1930.
- Ivanova, P. T., S. B. Milne, and H. A. Brown. 2010. Identification of atypical ether-linked glycerophospholipid species in macrophages by mass spectrometry. *J. Lipid Res.* **51**: 1581–1590.
- Nagy, K., V. V. Brahmabhatt, O. Berdeaux, L. Bretillon, F. Destailats, and N. Acar. 2012. Comparative study of serine-plasmalogens in human retina and optic nerve: identification of atypical species with odd carbon chains. *J. Lipid Res.* **53**: 776–783.
- Hanada, K. 2018. Lipid transfer proteins rectify inter-organelle flux and accurately deliver lipids at membrane contact sites. *J. Lipid Res.* **59**: 1341–1366.